

Elastic modulus of crystalline regions of poly(ether ether ketone), poly(ether ketone) and poly(*p*-phenylene sulphide)

Takashi Nishino, Kazuhiro Tada and Katsuhiko Nakamae*

Department of Industrial Chemistry, Faculty of Engineering, Kobe University,
1 Rokko-dai, Nada, Kobe 657, Japan

(Received 9 November 1990; revised 13 February 1991; accepted 27 February 1991)

Elastic moduli E_1 of crystalline regions in the direction parallel to the chain axis were measured by X-ray diffraction for poly(ether ether ketone) (PEEK), poly(ether ketone) (PEK) and poly(*p*-phenylene sulphide) (PPS). E_1 values of 71 GPa, 57 GPa and 28 GPa were obtained for PEEK, PEK and PPS, respectively. The calculated values for Treloar's method agreed well with these observed E_1 values. These small E_1 values were considered to be due to the fact that the lengths of the arms where the moment of force acts during the deformation are longer for these polymers than for polyethylene (PE). The deformation through bond angle bending at hetero atoms played an important contribution to the extension of the chains. The difference in E_1 values among these polymers was found to depend on the difference in the bond angles and their force constants. Elastic moduli E_t of crystalline regions in the direction perpendicular to the chain axis were also measured for PEEK and PEK. These E_t values were somewhat larger than those for PE; however, strong intermolecular interactions were not considered to act in these polymers. The intermolecular cohesive energy and heat resistance of these super engineering plastics were able to be evaluated through the measurement of E_t values.

(Keywords: crystal modulus; poly(ether ether ketone); poly(ether ketone))

INTRODUCTION

The elastic moduli of polymer crystals provide us with important information on the molecular conformation and intermolecular forces in the crystal lattice, and on the relation of these to the mechanical properties of polymers¹⁻⁶. We have been engaged in measuring the elastic modulus of crystalline regions of various polymers in the directions parallel (E_1) and perpendicular (E_t) to the chain axis by X-ray diffraction¹⁻⁶. Examination of the data so far accumulated led us to success in relating the E_1 value—viz. the extensivity of a polymer molecule—to the molecular conformation and the deformation mechanism of a polymer molecule in the crystal lattice. The values of E_1 for polymers with a fully extending planar zigzag conformation, e.g. polyethylene (PE) and poly(vinyl alcohol) (PVA), were found to be 235 and 250 GPa, respectively. Knowing of the elastic modulus E_1 of crystalline regions of polymers is also of importance in connection with the mechanical properties of polymers, because E_1 gives us the maximum value for the specimen modulus of a polymer. On the other hand, the elastic modulus E_t gives information on the intermolecular forces and their anisotropy. The value of E_t varies from 11.4 GPa for nylon 6 γ -form (intermolecular hydrogen bonds acting) to 2 GPa for isotactic poly-1-butene (van der Waals force acting).

Recently, many engineering plastics have been developed for wide practical usages as industrial and structural materials. In particular, poly(ether ether ketone) (PEEK),

poly(ether ketone) (PEK) and poly(*p*-phenylene sulphide) (PPS) are in the limelight as super engineering plastics, because they are easy to process and have extremely high heat resistance and chemical resistance⁷. They are polymers in which para-positions of phenyl rings are linked with various atoms or groups (O, CO, S), and are reported to be crystalline polymers whose skeletons have a zigzag conformation in the crystalline regions⁸. PPS is also known to form electrically conducting complexes upon doping with electron acceptors or donors⁹.

In this paper, we measured the E_1 values for PEEK, PEK and PPS and the E_t values for PEEK and PEK by X-ray diffraction, and then investigated the relationships between the mechanical properties, the conformation of molecular chains, and the intermolecular interactions of these polymers.

EXPERIMENTAL

Samples

A PEEK film (Sumitomo Chemical Co., Ltd, thickness 150 μm) was drawn 4 times at 170°C and kept at that length while being annealed at 300°C for 1 h. A PEK film, which had been previously drawn 4 times uniaxially, was drawn 1.2 times at 200°C and kept at that length while being annealed at 320°C for 1 h. PPS fibres (Toray Industries, Inc., fibre diameter 17 μm) were annealed at 250°C for 1 h at constant length.

* To whom correspondence should be addressed

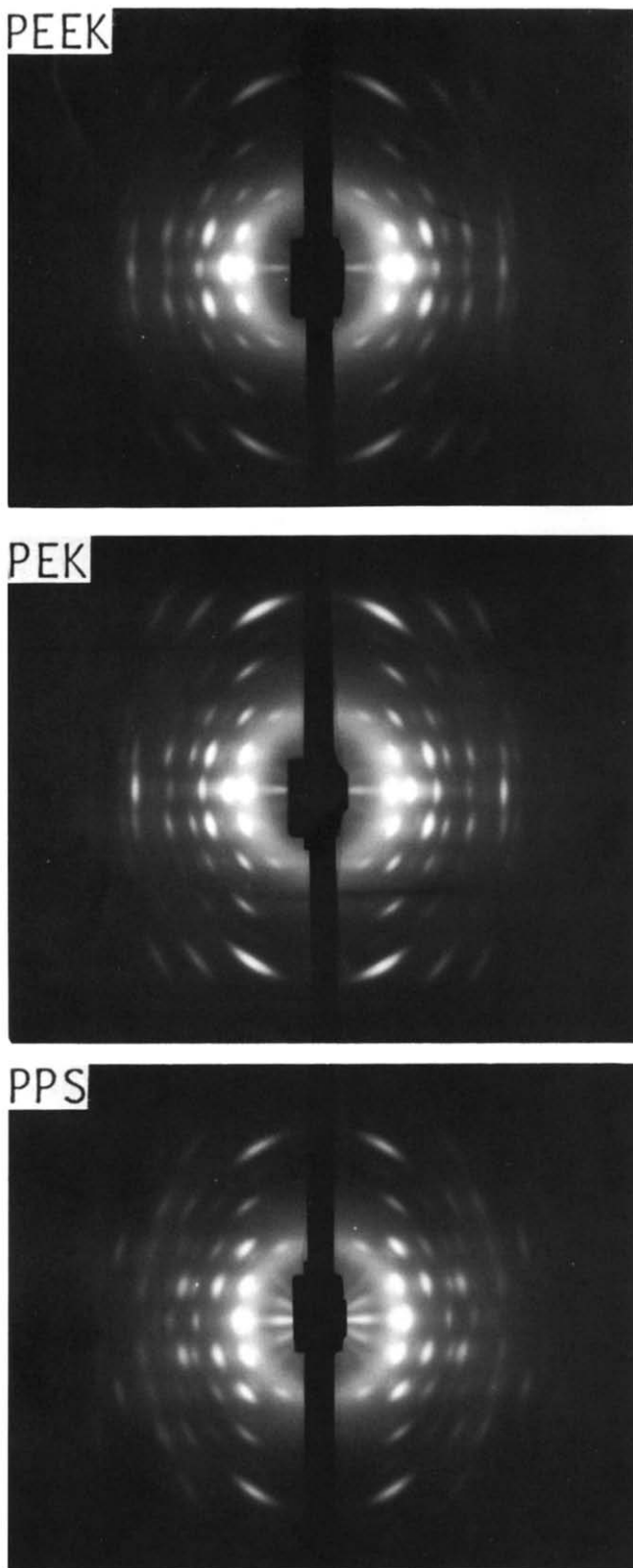


Figure 1 X-ray fibre photographs of poly(ether ether ketone), poly(ether ketone) and poly(*p*-phenylene sulphide)

Lattice parameter

Figure 1 shows an X-ray fibre photograph of each sample at room temperature. All specimens showed high crystallinity and a high degree of orientation of crystalline regions. X-ray fibre photographs were taken by using a cylindrical camera (radius 34.9 mm) with Ni-filtered CuK_α radiation. The lattice parameters were determined

by drawing the reciprocal lattice rotation diagrams from the diffraction position of each spot. The number of diffraction spots were 23, 30 and 26 for PEEK, PEK and PPS, respectively. The precise fibre period (the fibre axis is 'c' in all cases) was determined from the lattice spacing of the 008 reflection by using a wide-angle X-ray diffractometer (Rigaku Denki RAD-B System). The spacings were calibrated by the spacings of reflections of LiF.

Density

The density d of the specimen was obtained by a flotation method (benzene-carbon tetrachloride system) at 30°C. The degree of crystallinity X_c was calculated by the following equation:

$$1/d = X_c/d_c + (1 - X_c)/d_a \quad (1)$$

where d_c is the crystal density and d_a is the amorphous density^{8,10,11}

Melting point and heat of fusion

The melting point T_m and the heat of fusion ΔH of each sample were measured using a differential scanning calorimeter (Daini Seikosha, SSC-560S) at a sample weight of ca. 10 mg, and a heating rate of 10°C min⁻¹. T_m and ΔH were determined as a peak temperature and area of the whole melting endotherm, respectively.

Specimen modulus

The macroscopic specimen modulus Y_1 was measured from the initial slope of the stress-strain curve by using a tensile tester (Simadzu, Autograph IS-100) at 25°C. The initial length of the specimen was 20 mm, and the extension rate was 2 mm min⁻¹. At the same time, the tensile strength and the elongation at break were also measured.

Degree of orientation

The degree of orientation π was defined by

$$\pi = (180 - H^\circ)/180 \quad (2)$$

where H° is the half-width of the intensity distribution curve for the 008 reflection of each sample along the Debye-Scherrer ring.

Crystallite size

Determination of the crystallite size D and the lattice distortion of each sample along the chain direction was performed by measuring the meridional profiles of the 002, 006 and 008 reflections for PEEK and PEK, and the 002, 004, 006 and 008 reflections for PPS. The observed integral width β of each reflection was corrected for both the CuK_α doublet broadening (Jones' method) and the instrumental broadening b according to the equation:

$$\beta^2 = B^2 - b^2 \quad (3)$$

where β is the pure integral width of each reflection. The integral width (δS) in the reciprocal lattice space was given as follows:

$$(\delta S) = \beta \cos \theta / \lambda \quad (4)$$

where θ is the Bragg angle and λ is the X-ray wavelength.

It has been said that there are two types of lattice distortions, that is, the microcrystalline type distortion

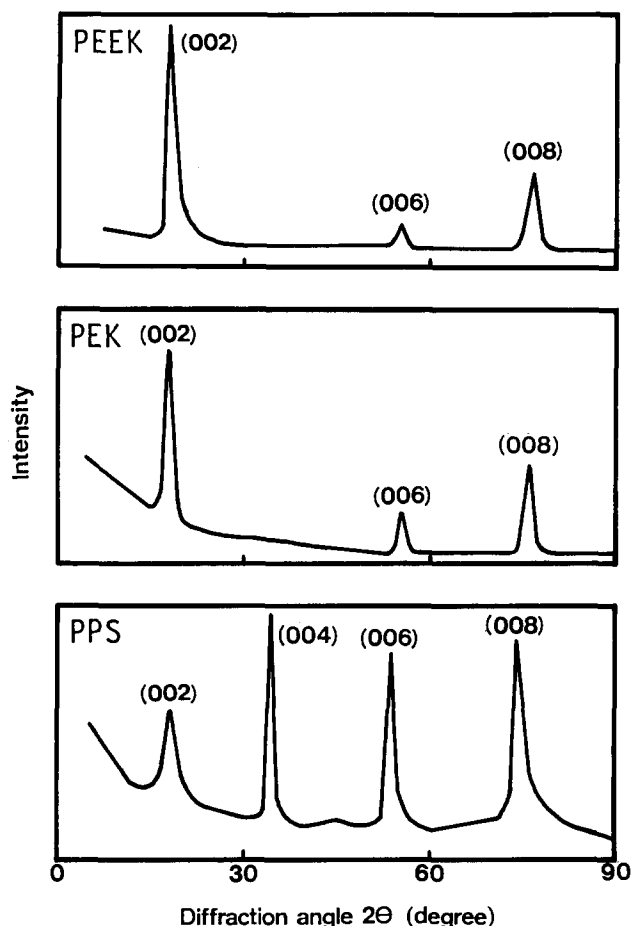


Figure 2 Meridional diffraction patterns of poly(ether ether ketone), poly(ether ketone) and poly(*p*-phenylene sulphide)

(the first kind) and the paracrystalline type distortion (the second kind). In preliminary experiments, we confirmed there were paracrystalline type distortions in these three polymers. Here the parameter of paracrystalline type distortion g_{11} was calculated as follows¹²:

$$(\delta S)^2 = (1/D^2) + (\pi^4 g_{11}^4 m^4 / d^2) \quad (5)$$

where m is the order of reflections and d is the fibre identity period. Then the crystallite size D and the parameter of paracrystalline distortion g_{11} in the direction parallel to the chain axis were obtained from the intercept and slope of the $(\delta S)^2$ versus m^4 plots.

The crystallite size $D_{(hk0)}$ of each sample in the direction perpendicular to the chain axis was obtained from the 200 and 020 reflections by using equation (4) and Scherrer's equation.

Long period

Small angle X-ray scattering was measured with a small-angle X-ray diffractometer (Rigaku Denki, with slit collimation; sample-counter distance: 300 nm). After background reduction, the long period L along the chain axis was measured by adopting the Bragg equation to the first peak position of the scattering profile.

Elastic modulus of crystalline regions

Figure 2 shows the meridional diffraction patterns of PEEK, PEK and PPS. Three or four meridional reflections were observed and they were able to be indexed as shown in the figure. All the reflections were

used for the measurement of E_1 . On the other hand, the reflections used for the measurement of E_t were three equatorial reflections (110, 200 and 020), which strongly appeared in the low angle region in Figure 1.

The lattice extension under a constant load was measured by means of an X-ray diffractometer equipped with a stretching device and a load cell. The strain ε in the crystalline regions was estimated by use of the relation:

$$\varepsilon = \Delta d / d_0 \quad (6)$$

where d_0 denotes the initial lattice spacing, and Δd is the change in lattice spacing induced by a constant stress. The experimental error in measuring the peak shift was evaluated ordinarily to be less than $\pm 0.01^\circ$ in 2θ angle.

The stress σ in the crystalline regions was assumed to be equal to the stress applied to the sample. This assumption of homogeneous stress distribution has been proven experimentally for PE, PVA, cellulose^{1-3,13,14}, poly(ethylene terephthalate)¹⁵, poly(*p*-phenylene terephthalamide)¹⁶, isotactic poly(4-methyl-pentene)¹⁷ etc.

The elastic moduli E_1 and E_t were calculated as:

$$E = \sigma / \varepsilon \quad (7)$$

Here σ and ε were not corrected for inclination of the lattice plane, because in this study we used the meridional reflections. A more detailed description of the measurements was given in earlier papers^{1-6,13,14}.

RESULTS AND DISCUSSION

Characterization of samples

Table 1 shows some characteristics of PEEK, PEK and PPS. Though all polymers had high melting points as expected for heat resistant polymers, all other properties such as crystallinity, specimen modulus, etc. of these polymers were approximately the same as those of conventional polymers. Crystallite sizes along the chain axis were small and were only several times longer than the fibre identity periods.

As shown in Figure 1, X-ray fibre photographs of PEEK, PEK and PPS resemble one another. All the polymers belong to an orthorhombic unit cell with the space group of $Pbcn-D_{2h}^{14}$, and the a , b and c dimensions

Table 1 Physical data for poly(ether ether ketone), poly(ether ketone) and poly(*p*-phenylene sulphide)

	PEEK	PEK	PPS
Density (g cm ⁻³)	1.303	1.317	1.348
Crystal density (g cm ⁻³)	1.382 ¹⁰	1.430 ¹¹	1.430 ¹¹
Amorphous density (g cm ⁻³)	1.265 ⁸	1.272 ¹¹	1.320 ¹¹
Crystallinity (%)	34	31	27
Melting point (°C)	343	375	289
Heat of fusion (cal g ⁻¹)	7.67	9.96	6.97
Specimen modulus (GPa)	6.8	5.4	8.1
Elongation at break (%)	25.4	30.2	16.6
Tensile strength (MPa)	460	323	609
Degree of orientation (-)	0.955	0.963	0.965
Crystallite size a axis (Å)	65	69	46
b axis (Å)	76	50	89
c axis (Å)	90	77	82
Distortion (%)	1.11	0.89	1.42
Long period (Å)	143	136	113
Lattice parameter a axis (Å)	7.67	7.62	8.52
b axis (Å)	5.91	5.87	5.76
c axis (Å)	9.93	10.03	10.27

of one of the polymers are approximately equal to those of others^{10,11,18} (see Table 1). Though the crystallographic repeat period must be about 30 Å for PEEK, and 20 Å for PEK with two monomers, the fibre identity periods were ca. 10 Å without appearance of the diffraction peak corresponding to 15 Å or 30 Å for PEEK, and 20 Å for PEK. This means that the molecular chains of PEEK

and PEK are packed in the unit cell without distinguishing their ether and ketone groups. The bond angles at hetero-atoms which link the para-positions of phenyl rings are 126.5° for PEEK¹⁰ and PEK. On the other hand, the bond angle of PPS is somewhat small (110°). These unit cell parameters are in accordance with those previously reported^{10,11,18}.

Elastic modulus E_1 of crystalline regions

Figure 3 shows the stress σ -strain ϵ curves for the (008) plane of PEEK, PEK and PPS at room temperature. All the strains were reversible. The initial slopes of the curves increased in this order. This indicates that the molecules of PPS in the crystalline regions are the easiest to elongate. From these slopes, the E_1 values of 71 GPa, 57 GPa and 28 GPa were obtained for PEEK, PEK and PPS, respectively. The f -values, the force required to stretch a molecule by 1%, calculated from both the E_1 value and the cross-sectional area of one molecule in a crystal lattice, were 1.61×10^{-5} dyn, 1.27×10^{-5} dyn and 0.69×10^{-5} dyn for PEEK, PEK and PPS, respectively. The observed E_1 values were smaller than for other rigid polymers such as aromatic polyamides^{4,5,16} and aromatic polyesters^{4,5}. Accordingly, these polymers in question can be used as the matrix resins of high performance composite materials with their high heat resistances; however, high modulus materials cannot be obtained from them because their E_1 values, i.e. the maximum attainable moduli, are relatively small.

Figure 4 shows the skeletal structure of PEEK¹⁰. The E_1 values of the three polymers used in this study were very different from one another, though these polymers are reported to have essentially the same skeletal structure in which phenyl rings are incorporated as the skeletal arms in the large scale extended zigzag conformation. Moreover, the E_1 values and the f -values for these polymers are from one-third to one-tenth of those of PE and PVA, which have a fully extended planar zigzag conformation. These small E_1 values are considered to be owing to the fact that the arms, where the moment of force acts during the deformation, are longer for these polymers (PEEK and PEK, 5.0 Å; PPS, 5.1 Å) than that for PE (0.9 Å).

In order to investigate the difference in these E_1 values, we next calculated the E_1 values for PEEK, PEK and PPS by Treloar's method²⁰. The bond lengths and bond angles and their force constants are shown in Table 2^{10,20-22}. The calculated values of E_1 for PEEK, PEK and PPS were 60 GPa, 52 GPa and 26 GPa, respectively. These values agreed well with the observed E_1 .

Figure 5 shows the mean distribution of the atomic displacement in each molecule when the molecule is

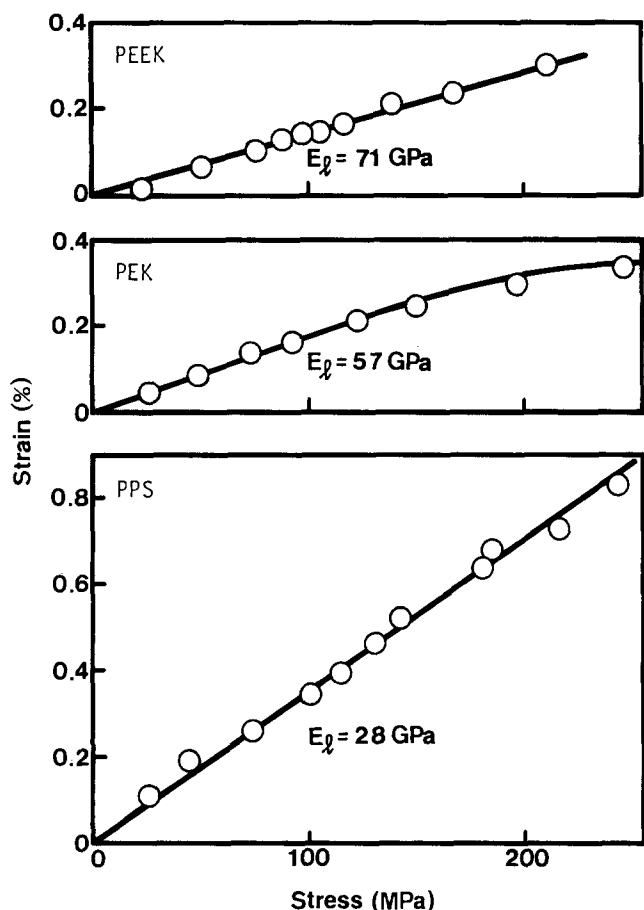


Figure 3 Stress-strain curves for the (008) plane of poly(ether ether ketone), poly(ether ketone) and poly(*p*-phenylene sulphide)

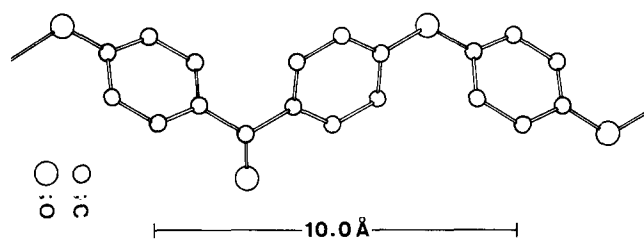


Figure 4 Skeletal structure of poly(ether ether ketone)

Table 2 Stretching and bending force constants

Bond	Stretching		Bending		
	Bond distance (Å)	Force constant k_1 (10^2 (N m))	Angle	Bond angle (degree)	Force constant k_p (10^2 (N m ⁻¹))
C-O	1.47 ¹⁰	4.54 ²⁰	C-O-C	126.5 ¹⁰	0.54 ³³
C-C	1.47 ¹⁰	3.70 ²²	C-C(O)-C	126.5 ¹⁰	0.15 ²²
C-S	1.74	2.43 ²²	C-S-C	110.0 ¹⁸	0.157 ²²
C _{aro} -C _{aro}	1.39 ³²	7.62 ²¹	C _{aro} -C _{aro} -C _{aro}	-	0.661 ²²
				-	1.06 ²⁰

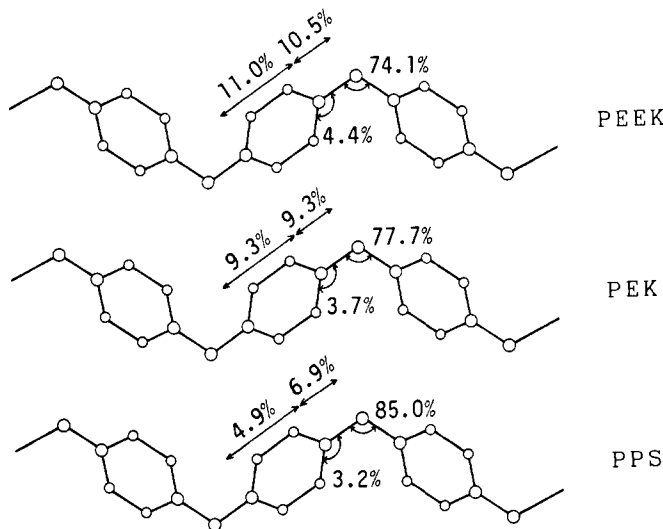


Figure 5 Deformation distribution in each molecule for total tensile strain of 100%

Table 3 Elastic modulus E_1 of poly(*p*-phenylene sulphide) calculated with changing bond angle ph-S-ph

ψ (degree)	C-S (Å)	E_1 (calc) (GPa)
103	1.89	24
110	1.74	26
120	1.57	31
126.5	1.48	35

stretched. The deformation through bond angle bending at hetero-atoms plays an important contribution to the extension of the chain. The bending force constant for the ketone group is one-third of that for the ether group. This is the reason the E_1 value of PEK, whose ketone content is larger than for PEEK, is smaller than that of PEEK. For PPS, both the small bending force constant for sulphide and the small bond angle bring the much smaller E_1 value. Garbarczyk reported the bond angle of sulphide from 103° to 107° ²³ instead of 110° ¹⁸ based on the potential energy calculation. So E_1 was calculated for these bond angles under the restriction of the fibre identity period being fixed at the observed value (10.27 Å).

Table 3 shows the change in the calculated E_1 value with the bond angle. It is evident that the bond angle greatly affects the E_1 value. A small bond angle gave a small E_1 value and diverged from the observed E_1 value. As a result, the calculated E_1 value for the bond angle of 110° fits the observed E_1 value. Thus, the bond angle of PPS seems to be near 110° from the mechanical point of view, too.

Macroscopic specimen moduli Y_1 are relatively small for these polymers. For example, Kunugi *et al.* reported a Y_1 value of PEEK up to 13.3 GPa by zone-drawing, which corresponds to 19% of E_1 ²⁴. As far as we know, this is the maximum attained Y_1 for PEEK. As described before, E_1 values, which are the maximum attainable moduli, were relatively small and this limited Y_1 values for the polymers mentioned here. Thus these small Y_1 seem to be ascribed partly to the small E_1 values.

Recently, Ward *et al.* reported the value of E_1 for PPS by X-ray diffraction²⁵. They obtained 38 GPa and 43 GPa for the observed and calculated E_1 values, respectively. They employed the (114) plane for the

measurement of E_1 , though the normal of this plane is inclined at 28.3° to the fibre axis and there are meridional reflections. They corrected the measured strain by considering this inclination of the plane, and the Poisson's ratio of the crystal lattice. Though full details are not known, the observed strain was multiplied by 0.7 in order to convert it to the value in the chain direction. We here measured the E_1 value for the (114) plane, and 32 GPa was obtained. By correcting the stress and strain simply with the inclination for the (114) plane, in this study, an E_1 value of 28 GPa was estimated for PPS. This value agrees with the E_1 value for the (008) plane. Thus, the correction method employed by Ward *et al.* seems not to be adequate.

As shown in Figure 2, there are some equivalent meridional reflections other than the 008 reflection. We then measured the E_1 value by using these planes in the same way.

Figures 6 and 7 show the σ - ϵ curves for the (002) and (006) planes of PEEK and PEK, respectively. Figure 8

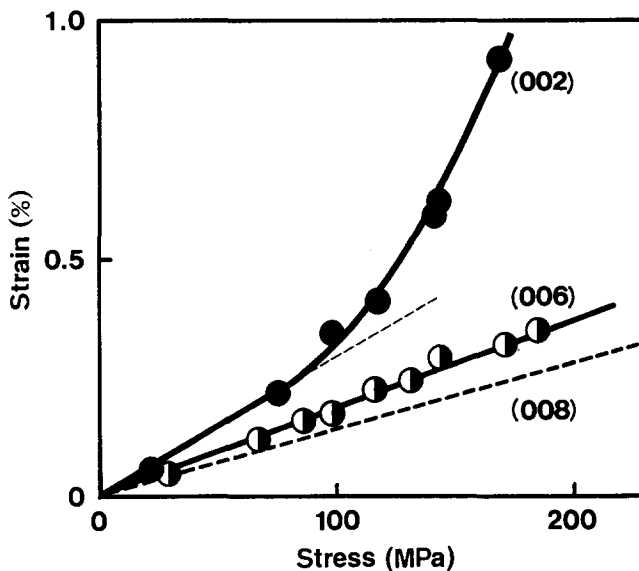


Figure 6 Stress-strain curves for the meridional reflections (●) (002) and (○) (006) planes of poly(ether ether ketone). Broken line, (008), indicates the results from Figure 3

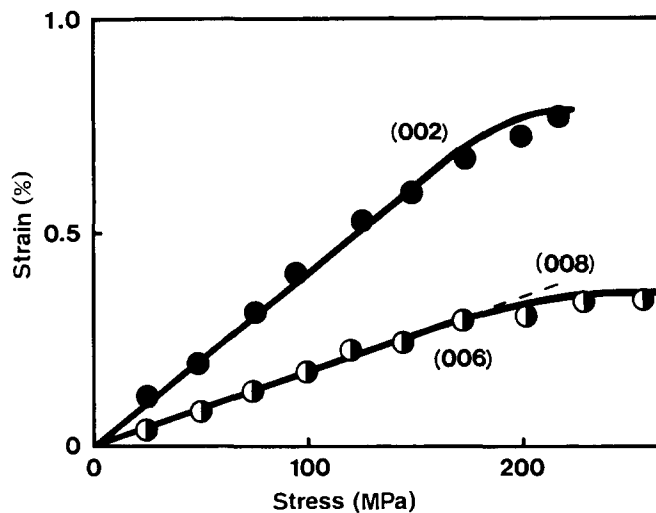


Figure 7 Stress-strain curves for the meridional reflections (●) (002) and (○) (006) planes of poly(ether ketone). Broken line, (008), indicates the results from Figure 3

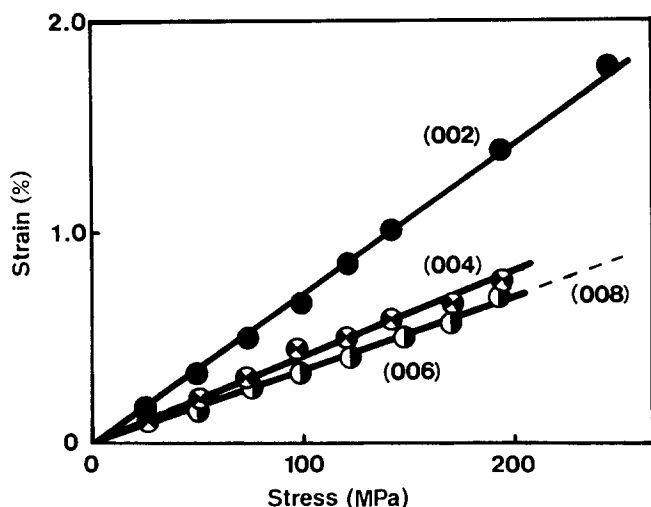


Figure 8 Stress-strain curves for the meridional reflections (●) (002), (●) (004) and (●) (006) planes of poly(*p*-phenylene sulphide). Broken line (008), indicates the results from Figure 3

shows the σ - ϵ curves for the (002), (004) and (006) planes of PPS. In all figures, the broken lines indicate the σ - ϵ curves for the (008) plane. The σ - ϵ curves for the (002), (004) and (006) planes differed from that for the (008) plane. The initial slope increased with a decrease in the order of reflections. This means that the E_1 value changed depending only on the order of reflection.

Table 4 shows the E_1 values obtained from the initial slopes of these curves and the fibre identity period measured for each meridional reflection of PEEK, PEK and PPS. Higher order reflections gave the higher E_1 values, though an inherent E_1 value should be obtained independent of the order of reflection. Similar phenomena were also observed for nylon 6 α -form^{26,27} and poly(*p*-benzamide)²⁸. In nylon 6 α -form, the E_1 value for the (040) plane (fibre axis 'b') was 53 GPa, but that for the (0140) plane was 183 GPa. When the crystallite size along the chain direction is small and changes with the applied stress, the diffraction peak shifts not only with the lattice extension, but also with the change in the Laue lattice factor. In most cases, the peak shift owing to the Laue lattice factor is negligible. However, the difference in E_1 values for nylon 6 was found to be due to the change of Laue lattice factor induced by the increase in the crystallite size with the applied stress. By correcting for the Laue lattice factor, the E_1 values measured for the different reflections agreed with each other^{26,27}. Warner reported that the fibre identity period determined from each meridional reflection did not agree with each other owing to the Laue lattice factor, when the number of the sub-period in one unit cell (in the case of nylon 6 α -form it corresponds to the number of methylene groups) is larger than the number of the unit cell in a crystallite, and the crystallite size is very small²⁹. The chemical structure of PEEK is $-(\text{O}-\text{C}_6\text{H}_4-\text{O}-\text{C}_6\text{H}_4-\text{CO}-\text{O}-\text{C}_6\text{H}_4)_n$ and the crystallographic repeat period should be ca. 30 Å. The observed crystallite size was 90 Å. In this case, the number of the sub-period ($-\text{O}-\text{C}_6\text{H}_4-\text{O}-$ or $-\text{O}-\text{C}_6\text{H}_4-\text{CO}-$) is twice as large as that of the unit cell.

From Table 4, the fibre identity period of each sample disagreed with one another. The higher order reflection gave both the higher E_1 value and the longer fibre identity period. Further, the lattice plane which gave nearly the same fibre period provided the same E_1 value. Accordingly,

it seems that the disagreement of the E_1 value for each reflection is due to the change in Laue lattice factor accompanied with the increase of crystallite size along the chain direction under stress. Consequently, we adopt the E_1 value for the (008) plane as both an accurate and reliable value for these polymers at room temperature.

Elastic modulus E_1 of crystalline regions

Figure 9 shows the σ - ϵ curves for the (110), (200) and (020) planes of PEEK and PEK, respectively. Though, in some cases, the curves deviated from an initial straight line at a high stress region, again all the strains were reversible. From the initial slopes, the E_1 values were obtained as follows:

PEEK 110: $E_1 = 5.9$ GPa	PEK 110: $E_1 = 5.4$ GPa
200: $E_1 = 4.2$ GPa	200: $E_1 = 5.6$ GPa
020: $E_1 = 5.0$ GPa	020: $E_1 = 5.7$ GPa

The E_1 values were smaller than the E_1 values described before by more than one order. While polymer main chain atoms are linked with covalent bonds, the auxiliary valences such as van der Waals force and hydrogen bonding act in the direction perpendicular to the chain axis as intermolecular interaction. This leads to smaller values for E_1 . These E_1 values are somewhat larger than that of PE (ca. 4 GPa)²⁰ at room temperature, but are smaller than those of nylon 6 γ -form in the hydrogen bonds direction (11.4 GPa)⁶ and polyoxymethylene in which dipole-dipole interaction acts (7.8 GPa)⁶. Thus strong intermolecular interaction was not considered to act in the polymers studied in this paper.

Figure 10 shows the anisotropies of E_1 in the *ab* plane of PEEK and PEK superposed on the crystal structure of PEEK. In order to draw the curves fitted to the observed values, the elastic modulus E_θ in the θ direction from the *a* axis was calculated as follows³¹:

$$1/E_\theta = (\cos^4 \theta/E_a) + (\sin^4 \theta/E_b) + \{(1/G_{ab}) - 2(v_{ab}/E_a)\} \sin^2 \theta \cos^2 \theta$$

where θ is the angle from the *a* axis, E_a and E_b represent the E_1 values for the (200) and (020) planes, respectively, G_{ab} and v_{ab} are the shear modulus and Poisson's ratio of the crystal lattice when stress is applied in the direction of the *a* axis. We here assumed v_{ab} to be 1/3. The area surrounded by the closed curve can be said to correspond to the integral of the intermolecular interaction in the direction perpendicular to the chain axis. Thus this may be regarded as one parameter for the intermolecular cohesive energy. Comparing these areas for PE³⁰, PEEK and PEK against one another, their ratio is 5.9:10:11.

The melting point of a polymer is defined as the ratio of the change in enthalpy to that in entropy on fusion

Table 4 Elastic modulus E_1 and fibre identity period *d* of poly(ether ether ketone), poly(ether ketone) and poly(*p*-phenylene sulphide)

	PEEK		PEK		PPS	
	E_1 (GPa)	<i>d</i> (Å)	E_1 (GPa)	<i>d</i> (Å)	E_1 (GPa)	<i>d</i> (Å)
(008)	71	9.93	57	10.03	28	10.28
(006)	55	9.94	57	10.03	29	10.27
(004)	*	*	*	*	24	10.27
(002)	31	9.84	25	9.91	14	10.09

* (004) reflections were not observed for poly(ether ether ketone) and poly(ether ketone)

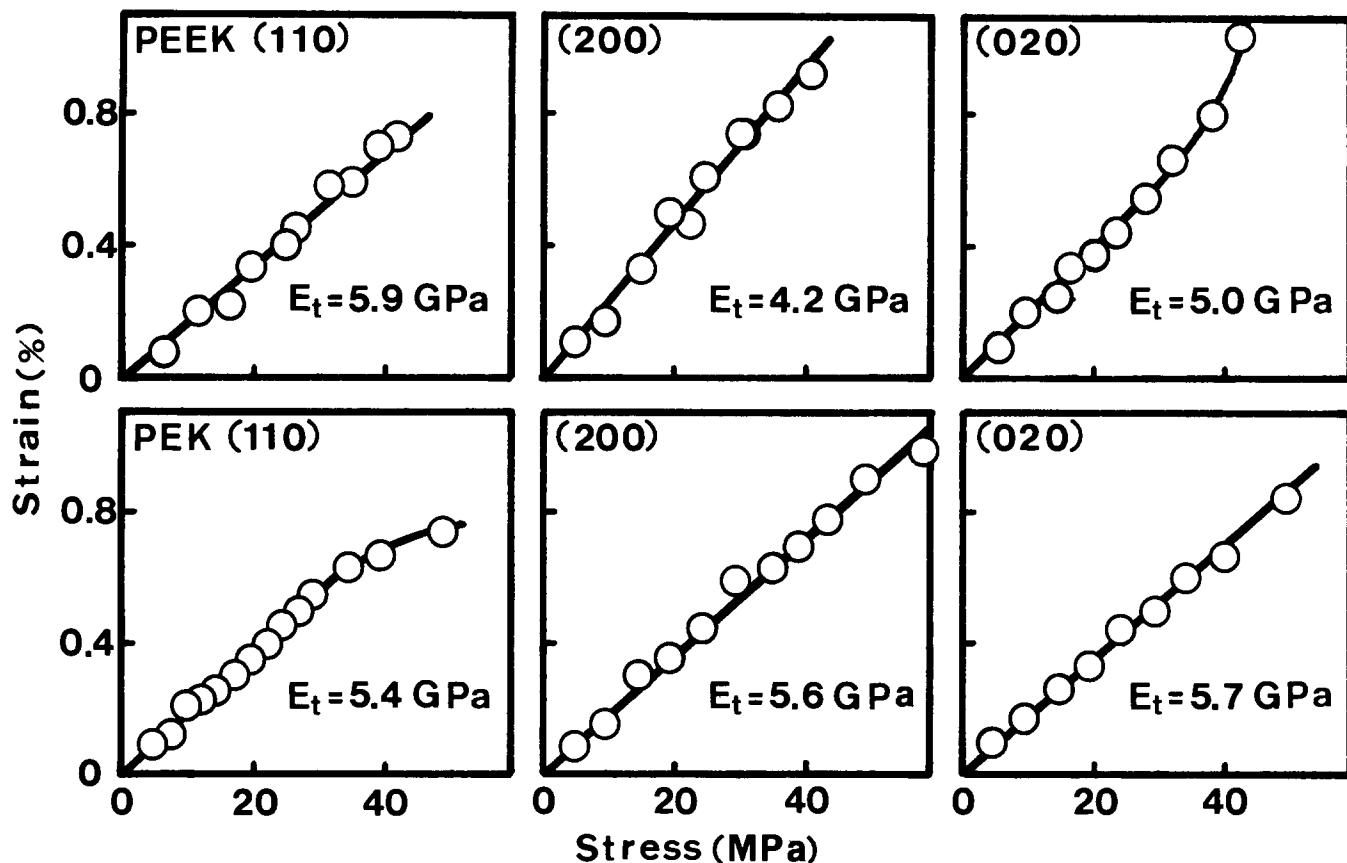


Figure 9 Stress-strain curves for the equatorial reflections of poly(ether ether ketone) and poly(ether ketone)

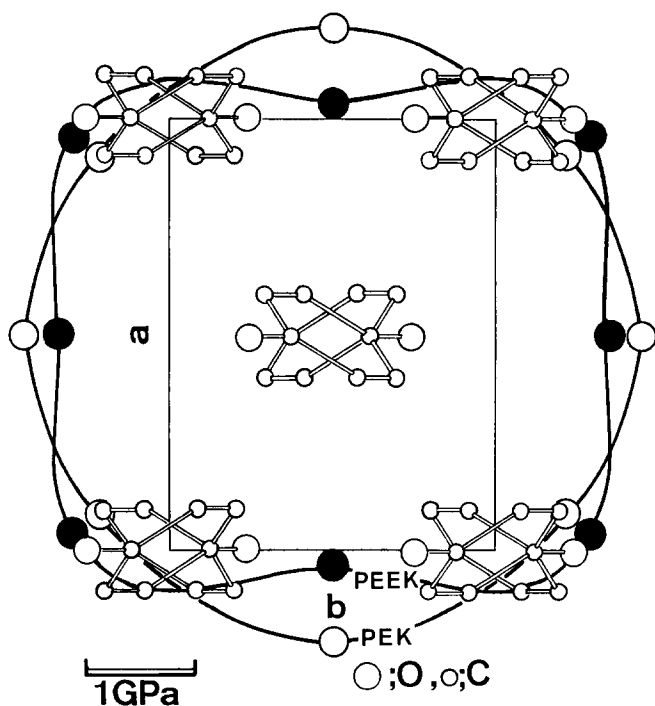


Figure 10 Anisotropies of elastic modulus E_t in the ab plane of poly(ether ether ketone) and poly(ether ketone)

and all these polymers have a zigzag skeletal conformation. In other words, T_m is considered to become the same parameter for the intermolecular cohesive energy in these cases. Considering the ratio for T_m of these polymers (PE, 418 K; PEEK, 621 K; PEK, 646 K) is 6.4:10:10.4, this ratio is nearly in accordance with that of the area

surrounded by the closed curves in Figure 10. Thus this resemblance indicates that T_m for these polymers is governed by the intermolecular cohesive energy. Accordingly, isotropic large intermolecular interaction (though there is no special strong interaction) is the reason why poly(aryl ether ketone)s have higher melting temperatures and are known as heat resistant polymers. Conversely, E_t values can provide important information on the heat resistivity of polymers.

The macroscopic specimen modulus Y_t in the direction perpendicular to the chain axis was 3.1 GPa for PEEK and 3.4 GPa for PEK. The ratios of the Y_t value to the E_t value, Y_t/E_t , are 0.53–0.74. These values are relatively large compared with other common polymers, where Y_t/E_t is usually less than 0.5. This indicates that the mechanical properties of these polymers are strongly controlled by that of crystalline regions in the normal direction.

REFERENCES

- 1 Sakurada, I., Nukushina, Y. and Ito, Y. *J. Polym. Sci.* 1962, **57**, 651
- 2 Sakurada, I., Ito, T. and Nakamae, K. *J. Polym. Sci. (C)* 1966, **15**, 75
- 3 Sakurada, I. and Kaji, K. *J. Polym. Sci. (C)* 1970, **31**, 57
- 4 Nakamae, K., Nishino, T., Shimizu, Y. and Matsumoto, T. *Polym. J.* 1987, **19**, 451
- 5 Nakamae, K. and Nishino, T. Proceedings of the 5th Rolduc Polymer Conference 1990, The Netherlands
- 6 Sakurada, I. and Kaji, K. *Makromol. Chem., Suppl.* 1975, **1**, 599
- 7 Attwood, T. E., Dawson, P. C., Freeman, J. L., Hoy, L. R. J., Rose, J. B. and Staniland, P. A. *Polymer* 1981, **22**, 1096
- 8 Dawson, P. C. and Blundell, D. J. *Polymer* 1980, **21**, 577

- 9 Chance, R. R., Schacklette, L. W., Miller, G. G., Ivory, D. M., Sowa, J. M., Elsenbaumer, R. L. and Baughman, R. H. *J. Chem. Soc. Chem. Comm.* 1980, 347
- 10 Shimizu, J., Kikutani, T., Ookoshi, Y. and Takaku, A. *Sen-i Gakkaishi* 1985, **41**, T-461
- 11 Harris, J. E. and Robeson, L. M. *J. Polym. Sci., Polym. Phys. (B)* 1987, **25**, 311
- 12 Hosemann, R. and Wilke, W. *Makromol. Chem.* 1968, **118**, 230
- 13 Sakurada, I., Ito, T. and Nakamae, K. *Makromol. Chem.* 1964, **75**, 1
- 14 Nishino, T., Ohkubo, H. and Nakamae, K. *J. Macromol. Sci.-Phys.* to be published
- 15 Nakamae, K., Nishino, T., Yokoyama, F. and Matsumoto, T. *J. Macromol. Sci.-Phys. (B)* 1988, **27**(4), 407
- 16 Nakamae, K., Nishino, T., Shimizu, Y., Hata, K. and Matsumoto, T. *Kobunshi Ronbunshu* 1986, **43**, 499
- 17 Nakamae, K., Nishino, T. and Takagi, S. *J. Macromol. Sci.-Phys.* in press
- 18 Tabor, B. J., Magre, E. P. and Boon, J. *Eur. Polym. J.* 1971, **7**, 1127
- 19 Nishino, T., Yokoyama, F., Nakamae, K. and Matsumoto, T. *Kobunshi Ronbunshu* 1983, **40**, 357
- 20 Treloar, L. R. G. *Polymer* 1960, **1**, 95, 279, 290
- 21 Shimizu, J., Kikutani, T., Ookoshi, Y. and Takaku, A. *Sen-i Gakkaishi* 1987, **43**, T-507
- 22 Mizushima, S. and Shimanouchi, T. 'Sekigai Kyusyu to Raman kouka (Infrared Absorption and Raman Effect)', Kyoritu Zensyo, Tokyo, 1987, p. 228
- 23 Garbacz, J. *Polym. Commun.* 1986, **27**, 335
- 24 Kunugi, T., Mizushima, A. and Hayakawa, T. *Polym. Commun.* 1986, **27**, 175
- 25 Unwin, A. P. and Ward, I. M. *Polym. Commun.* 1988, **29**, 250
- 26 Kaji, K. and Sakurada, I. *J. Polym. Sci., Polym. Phys. Edn.* 1974, **12**, 1491
- 27 Kaji, K. and Sakurada, I. *Makromol. Chem.* 1978, **179**, 209
- 28 Kaji, K. *Report of the Poval Committee* 1975, **66**, 113
- 29 Warner, L. G. *Monatsh. Chem.* 1948, **79**, 86, 279
- 30 Nakamae, K., Nishino, T., Hata, K. and Matsumoto, T. *Kobunshi Ronbunshu* 1986, **43**, 881
- 31 Odajima, A. and Maeda, T. *J. Polym. Sci. (C)* 1966, **15**, 55
- 32 Kakida, H., Chatani, Y. and Tadokoro, H. *J. Polym. Sci., Polym. Phys. Edn.* 1976, **14**, 427
- 33 Tadokoro, H., Chatani, Y., Yoshihara, T., Tahara, S. and Murahashi, S. *Makromol. Chem.* 1964, **73**, 109